International Immunopharmacology 14 (2012) 410–421

Contents lists available at SciVerse ScienceDirect

International Immunopharmacology

journal homepage: www.elsevier.com/locate/intimp

Glycyrrhizin regulates CD4$^+$T cell response during liver fibrogenesis via JNK, ERK and PI3K/AKT pathway☆

Chuan-tao Tu [a,1], Jing Li [b,1], Fu-ping Wang [a], Lei Li [a], Ji-yao Wang [a], Wei Jiang [a,*]

[a] Department of Gastroenterology, Zhongshan Hospital, Fudan University, Shanghai, China
[b] Department of Gastroenterology, Tongji Hospital, Tongji University, Shanghai, China

ARTICLE INFO

Article history:
Received 25 June 2012
Received in revised form 6 August 2012
Accepted 15 August 2012
Available online 30 August 2012

Keywords:
Glycyrrhizin
Liver fibrosis
CD4$^+$T cells
PI3K/AKT
MAPK/ERK
Concanavalin A

ABSTRACT

The aims of this study were to elucidate the immunomodulatory effects of glycyrrhizin (GL) on CD4$^+$T cell responses during liver fibrogenesis. To obtain in vivo evidence about the effects of GL on CD4$^+$T cells in livers and spleens of concanavalin A (ConA)-induced mouse model, mice were administrated with ConA together with or without GL for 8 weeks. Mice treated with GL dramatically prevented liver inflammation and fibrosis. Besides, GL inhibited the infiltration of T helper (Th) cell type 1, Th2, Th17 and regulatory T cells (Treg) in livers and spleens of mouse fibrosis models, and regulated the Th1/Th2 and Treg/Th17 balances respectively to a relative dominance of Th1 and Treg lineages in livers. Moreover, GL dramatically enhanced the antifibrotic cytokine interferon (IFN)-γ and interleukin (IL)-10. GL at a concentration of 10 or 100 μg/mL was respectively incubated with ConA-stimulated splenic CD4$^+$T cells in vitro, and JNK inhibitor (SP600125), ERK inhibitor (U0126), p38 inhibitor (SB203580) or PI3K/AKT inhibitor (LY29400225) was added during the incubation. Notably, GL not only inhibited ConA-induced proliferation of splenic CD4$^+$T cells but also enhanced the mRNAs of IFN-γ and IL-10 in these cells. Be similar to the effects of GL, SP600125, U0126 and LY29400225, however not SB203580, also inhibited ConA-induced CD4$^+$T cell proliferation, indicating the involvement of JNK, ERK and PI3K/AKT in this process. Moreover, GL significantly inhibited ConA-induced phosphorylation of JNK, ERK and PI3K/AKT in vitro. Collectively, GL might alleviate liver injury and fibrosis progression via regulation of CD4$^+$T cell response in JNK, ERK and PI3K/AKT-dependent pathways.

1. Introduction

Liver fibrosis and its end-stage cirrhosis represent the final common pathways of virtually all chronic liver diseases [1]. Chronic liver injury started by hepatitis virus infection or alcohol abuse usually arouse improper and persistent wound healing responses in liver, following by excessive deposition of extracellular matrix (ECM), the so-called liver fibrosis, and increased loss of liver function [1,2]. Hepatic stellate cells (HSCs) are the critical cells in liver fibrosis, orchestrating the deposition of ECM during liver fibrosis [3,4]. Cytokine-mediated activation of HSCs into a myofibroblast-like phenotype is a key event during liver fibrogenesis [2,4]. Although there is a great deal of mechanisms regarding the process of scar tissue formation [2,3], some big gaps are still in our understanding of the role of inflammatory cells and their cytokines in fibrogenesis.

Recently, accumulating evidence from mouse and human studies have emphasized the crucial role of infiltrating CD4$^+$T cells in the progression of liver inflammation and fibrosis [1,5–7]. It has become clear that CD4$^+$T cells have heterogeneous effects for the existence of diverse functional subsets [1,5–7]. CD4$^+$T helper cells have recently been subdivided into four major subsets, largely based on their expression profile of transcription factors and secreted cytokines: T helper (Th) cell type 1, Th2, Th17 and regulatory T cells (Tregs) [8,9].

The activity of HSCs is influenced by an array of cytokines, some of which are profibrotic, i.e. transforming growth factor (TGF)-β1, whereas others play an antifibrotic role, i.e. interleukin (IL)-10, interferon (IFN)-γ [3–7]. Moreover, HSCs with dual effects of antigen-presentation and collagen synthesis are recently reported to be involved in regulating CD4$^+$T cell responses [10,11]. Progressive carbon tetrachloride (CCl_4)-induced liver fibrosis in BALB/c mice is associated with increased levels of IL-4 and decreased levels of IFN-γ, synthesized by CD4$^+$ Th2 and CD4$^+$ Th1 cells, respectively [12]. Th1

☆ Funding: This study was supported by grants from the National Nature Science Foundation of China (No. 81070341) and Shanghai Nature Science Foundation (No. 09ZR1406000).

* Corresponding author at: Department of Gastroenterology, Zhongshan Hospital, Fudan University, 180 Fenglin Road, Shanghai 200032, China. Tel.: +86 21 64041990 2424; fax: +86 21 64432583.
E-mail addresses: tuchuantao@hotmail.com (C. Tu), lijingshengping@163.com (J. Li), 11211210011@fudan.edu.cn (F. Wang), li.lei@zs-hospital.sh.cn (L. Li), wang.jiyao@zs-hospital.sh.cn (J. Wang), jiang.wei@zs-hospital.sh.cn (W. Jiang).
[1] The two authors contribute equally to this paper.

1567-5769/$ – see front matter © 2012 Elsevier B.V. All rights reserved.
http://dx.doi.org/10.1016/j.intimp.2012.08.013

Table 1
Primer sequences used in this study.

Target genes	Forward primers(5′-3′)	Reverse primers (5′-3′)
GAPDH	TGTGTCCGTCGTGGATCTGA	TTGCTGTTGAAGTCGCAGGAG
A-SMA	AAGAGCATCCGACACTGCTGAC	AGCACAGCCTGAATAGCCACATAC
IFN-γ	GTTACTGCCACGGCACAGTCATTG	ATCCTTTTGCCAGTTCCTCCAG
TGF-β	GTGTGGAGCAACATGTGGAACTCTA	TTGGTTCAGCCACTGCCGTA
IL-10	GGTTGCCAAGCCTTATCGGA	ACCTGCTCCACTGCCTTGCT
IL-13	AGACCAGACTCCCCTGTGCA	TGGGTCCTGTAGATGGCATTG

dominance could result in virus clearance and always end with a process of acute HBV infection, whereas Th2 dominance could not clear virus and usually end with a process of chronic HBV infection [13]. Thus, the 'Th1/Th2 ratio' is ever used as an index to predict the outcome of virus infection and tilt the balance toward or away from fibrosis [12,13]. Besides, Treg cells induce immune tolerance, while Th17 cells mediate a strong inflammatory response [8,9]. Recently, it's reported that peripheral and hepatic Treg responses have been significantly enhanced in patients with chronic hepatitis B (CHB) and autoimmune hepatitis (AIH) [13,14], and also, Th17 cells significantly increased in CHB and AIH patients, which can activate mononuclear and dendritic cells to start the anti-viral immunity and prevent the apoptosis of virus-infected cells [15]. Nowadays, for the antagonistic functions of Treg and Th17 cells during HBV infection and their intrinsic developmental links [16], the significance of 'Treg/Th17 balance' has been frequently discussed in CHB pathogenesis [17,18].

Under inflammatory circumstances, the cytokines and growth factors in microenvironments could activate mitogen-activated protein kinase (MAPK) pathways in T cells [19,20]. So far, three distinct MAPK pathways have been described in mammalian cells: the extracellular signal-regulated kinase (ERK) pathway, the c-Jun amino terminal kinase (JNK) pathway and the p38 MAPK pathway [19]. Recent studies have also implicated that phosphatidylinositide 3-kinase (PI3K)/AKT pathway activation is a fundamental requirement for cell-cycle progression and T-cell proliferation [20]. MAPK/ERK and PI3K/AKT pathways are critical in transferring extracellular message via membrane-bound ligands, transmembrane receptors and cytoplasmic secondary messengers into cell nucleus, thus regulating the gene expression that controls several important cellular processes including cell proliferation and apoptosis are important targets for antifibrogenic treatments.

Glycyrrhizin (GL), the primary active constituent of licorice root, is commonly used in Asia to treat patients with chronic hepatitis [21–23]. GL could promote cell proliferation of hepatocytes thus it could be used to facilitate liver regeneration after liver injury. Besides, GL have anti-viral, anti-tumor and immunomodulatory abilities [24–26]. In patients with chronic hepatitis C, intravenous administration of GL could decrease plasma aminotransaminase levels, thus preventing liver fibrosis progression as well as subsequent hepatocellular carcinoma [22,27]. Our previous work had demonstrated that GL could prevent hepatotoxin-induced liver injury and cirrhosis via inhibition of NF-kappaB binding activity, cell proliferation and collagen production of HSCs [28]. However, the immunomodulatory activity of GL has not been fully elucidated in liver fibrosis. Here this study was designed both in vivo and in vitro to investigate whether GL could regulate $CD4^+$T cell response via JNK, ERK and PI3K/AKT signal pathways in mouse liver fibrosis models.

2. Materials and methods

2.1. Models of fibrosis and experimental design

Six-to-eight week old female BALB/c mice weighing 18–20 g were obtained from the Shanghai Laboratory Animal Centre (Chinese Academy of Science, Shanghai, China) and maintained under specific pathogen-free conditions with a 12-hour light/dark cycle and allowed free access to food and water. Concanavalin A (ConA) and glycyrrhizin (GL) were purchased from Sigma Chemical Co. (St. Louis, MO, USA) and dissolved in pyrogen-free phosphate buffered saline (PBS) and saline, respectively. Forty mice in each group were intravenously (i.v.) injected with ConA at a dose of 10 mg/kg body weight once a week for up to 8 weeks [29]. Control mice were injected with the same volume of PBS. Intraperitoneal administration of GL (10, 25, 50 mg/kg) or vehicle control (saline) was performed three times weekly after ConA treatment, respectively. The experimental procedures conforming to the guidelines outlined in the Guide for the Care and Use of Laboratory Animals and were approved by the Research Ethics Committee of Zhongshan Hospital (No. 2010-87).

Blood samples, liver and spleen specimens were collected at 24 h after weekly ConA administration at 0, 2, 4, and 8 weeks. Liver injury was determined by measuring serum alanine aminotransferase (ALT) levels using a commercially available Alanine Aminotransferase Reagent Kit (Rongsheng Biotech, Shanghai, China).

2.2. Histology

The harvested liver tissues were fixed in 10% neutral buffered formalin and embedded in paraffin. Slices 4 μm thick were prepared and stained with hematoxylin/eosin (H&E) and Masson's trichrome staining according to standard procedures. Fibrosis was graded on a 5-point scale based on Scheuer's scoring system [30], with 0 indicating no fibrosis; 1 indicating expansion of the portal tracts without linkage; 2 indicating portal expansion with portal linkage; 3 indicating extensive portal to portal and focal portal to central linkage; and 4 indicating complete cirrhosis. Histological assessment was performed by two clinical pathologists without knowledge of the experimental design.

2.3. Immunohistochemistry

The liver tissue sections were dewaxed, hydrated and subjected to heat-induced antigen retrieval. Sections were blocked and incubated overnight at 4 °C with mouse anti-α-SMA antibody (clone 1A4, Sigma-Aldrich) 1:100, and primary antibody diluted in TBS containing 2% bovine serum albumin. Negative-control antibodies consisted of species-matched and where appropriate, IgG subclass-matched Ig, used at the same dilution. The sections were subsequently washed and incubated with HRP-conjugated goat anti-mouse IgG secondary antibodies, followed by incubation for 5- to 10-min with 3, 3′-diaminobenzidine tetrachloride and visualization of specific staining under light microscopy.

2.4. Preparation of non-parenchymal cells from mouse livers and spleens

Livers and spleens were harvested at the indicated time points and pressed through a 200-gage stainless steel mesh and suspended in PBS. For the preparation of non-parenchymal hepatic cells, the abdominal cavities of anesthetized mice were opened and the livers

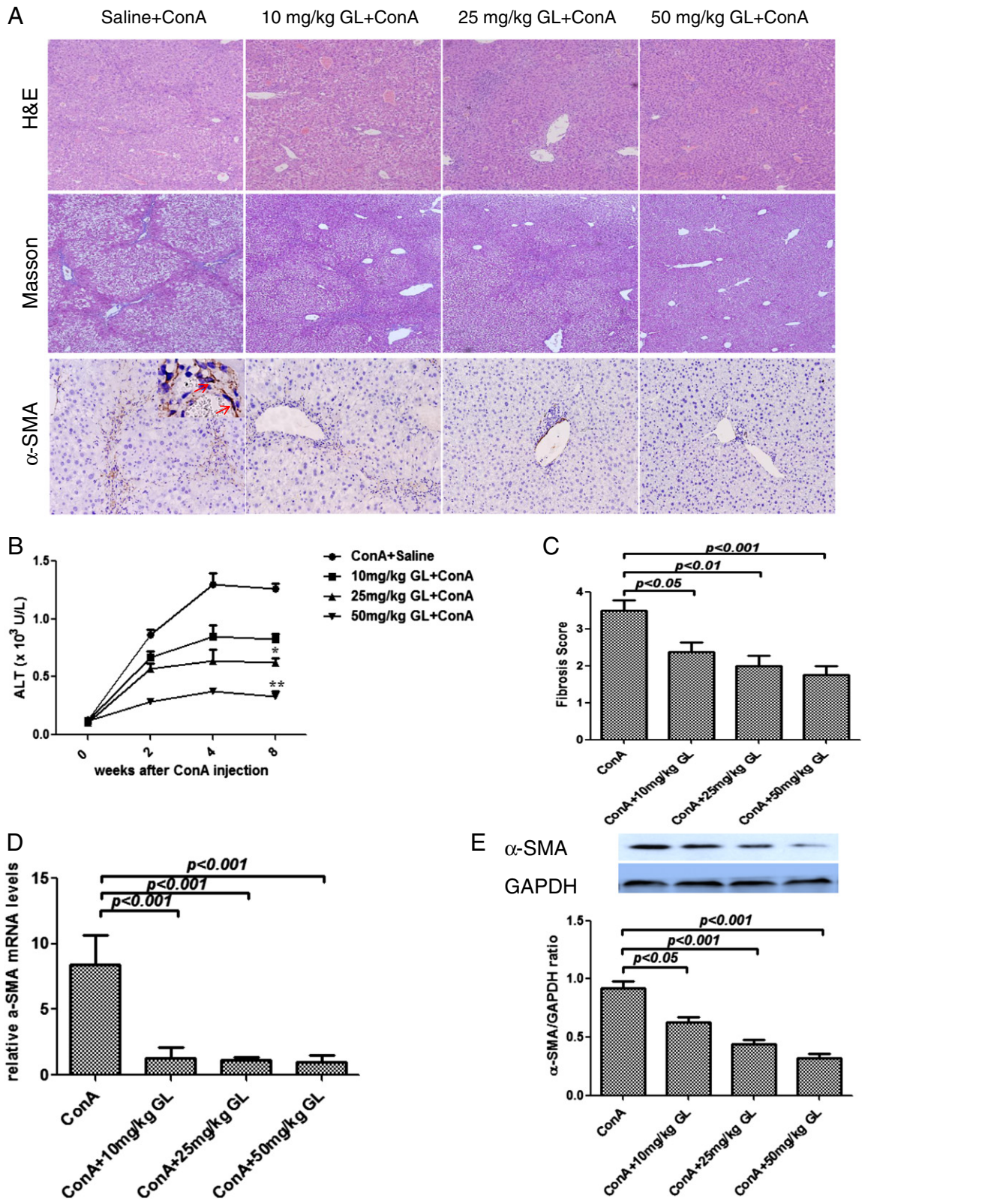

Fig. 1. Glycyrrhizin (GL) administration ameliorates ConA-induced hepatic injury, inflammation, and fibrogenesis in mouse models. (A) Histology was assessed by H&E staining and fibrillar collagen deposition was evaluated by Masson staining (original magnification, ×100). Activated HSCs were performed on liver sections by immunohistochemical staining of alpha-smooth muscle actin (α-SMA) (original magnification, ×200). The positive α-SMA staining in cytoplasm (red arrows) is mainly located around the pseudolobule. (B) Liver injury was assessed by serum ALT. Serum ALT levels at different time points after ConA injection with or without GL administration at different concentrations. $^{*}p<0.05$ for ConA + 25 mg/kg GL vs. ConA + Saline, $^{**}p<0.01$ for ConA + 50 mg/L GL vs. ConA + Saline (n = 10 per group). (C) Degree of liver fibrosis was assessed based on Scheuer's scoring system. (n = 8 per group). (D) The mRNAs of α-SMA in mouse liver tissues were analyzed by real-time PCR (n = 6 per group). Results were normalized to GAPDH expression. (E) The proteins of α-SMA in liver tissues at week 8 after ConA injections are presented as ratio of α-SMA/GAPDH. Representative blots were presented. Pooled data from 4 mice in each group are shown as mean ± SEM.

were perfused through the portal vein for 5 min with Hank's balanced salt solution (HBSS), 4 min with 0.5 mg/mL pronase solution, and 4 min with 0.25 mg/mL collagenase solution at a flow rate of 6 mL/min. The hepatic tissue was then minced and further digested in 50 mL HBSS supplemented with 50 mg collagenase, 50 mg pronase, and 1 mg DNase (20 min, 37 °C). The resulting cell suspension was passed through a 100 μm nylon mesh filter and then centrifuged at 300 *g* (10 min, 4 °C). The cell pellets were resuspended in 8 mL 40% Percoll solution and then carefully overlaid on 5 mL of 70% Percoll solution (Sigma-Aldrich, St. Louis, MO, USA). After centrifugation at 450 *g* (30 min, 17 °C), the layer of cells at the intermediate interface was harvested as target cells. Splenic cells were isolated following mechanical disruption of the spleen and erythrocyte lysis as described elsewhere [31].

2.5. Purification of $CD4^+$T cells

$CD4^+$T cells were purified from non-parenchymal cells of mouse livers and spleens using the Dynal® Mouse CD4 Cell Negative Isolation Kit (Invitrogen Dynal AS, Carlsbad, CA, USA) according to the manufacturer's protocol. After isolation, $CD4^+$T cells were resuspended in the respective supplemented RPMI-1640 medium (Gibco, Grand Island, NY, USA). Subsequently, cells were cryopreserved in a medium containing 75% FBS, 15% RPMI-1640 and 10% DMSO. The cells were thawed by a step-by-step, gradual dilution method. Cell viability was confirmed over 90% by Trypan blue exclusion.

2.6. Flow cytometry

All antibodies used in flow cytometry were purchased from eBioscience (San Diego, CA, USA). For the staining of intracellular cytokines such as IFN-γ, IL-4 and IL-17, cells were stimulated with phorbol-12-myristate-13-acetate (PMA, 25 ng/mL, Enzo, New York, NY, USA) and ionomycin (1 μg/mL, Enzo) in 1 mL RPMI 1640 medium supplemented with 10% FCS for 6 h. Brefeldin A (1 μg/mL, Enzo) was added 1 h prior to cell harvesting. After labeling with surface antibodies, cells were permeabilized with a fix/perm solution (eBioscience) and stained with the appropriate intracellular antibodies according to the manufacturer's instructions. Isotype-matched control antibodies were used to determine the level of background staining and help set a gate. Stained cells were analyzed by FACSCalibur (Becton Dickinson) and FlowJo software 7.6.1 (Tristar, El Segundo, CA, USA).

2.7. T-cell proliferation assay

Purified spleen $CD4^+$T cells were cultured in triplicate in a concentration of 1×10^5 cells per well in 100 μL RPMI 1640 containing 10% FCS. First, the cells were stimulated with or without10 μg/mL ConA for 0, 12, 24, 48 and 72 h. IL-2 (20 U/mL, PeproTech) was also added during the incubation to prevent the anergic state of T cells. Second, GL at different concentrations (0, 10, 100 μg/mL) was added to test the effect of GL on ConA-induced $CD4^+$ cell proliferation in vitro. Cell proliferation was measured using the thymidine method, and converted to a stimulation index, defined as the mean number

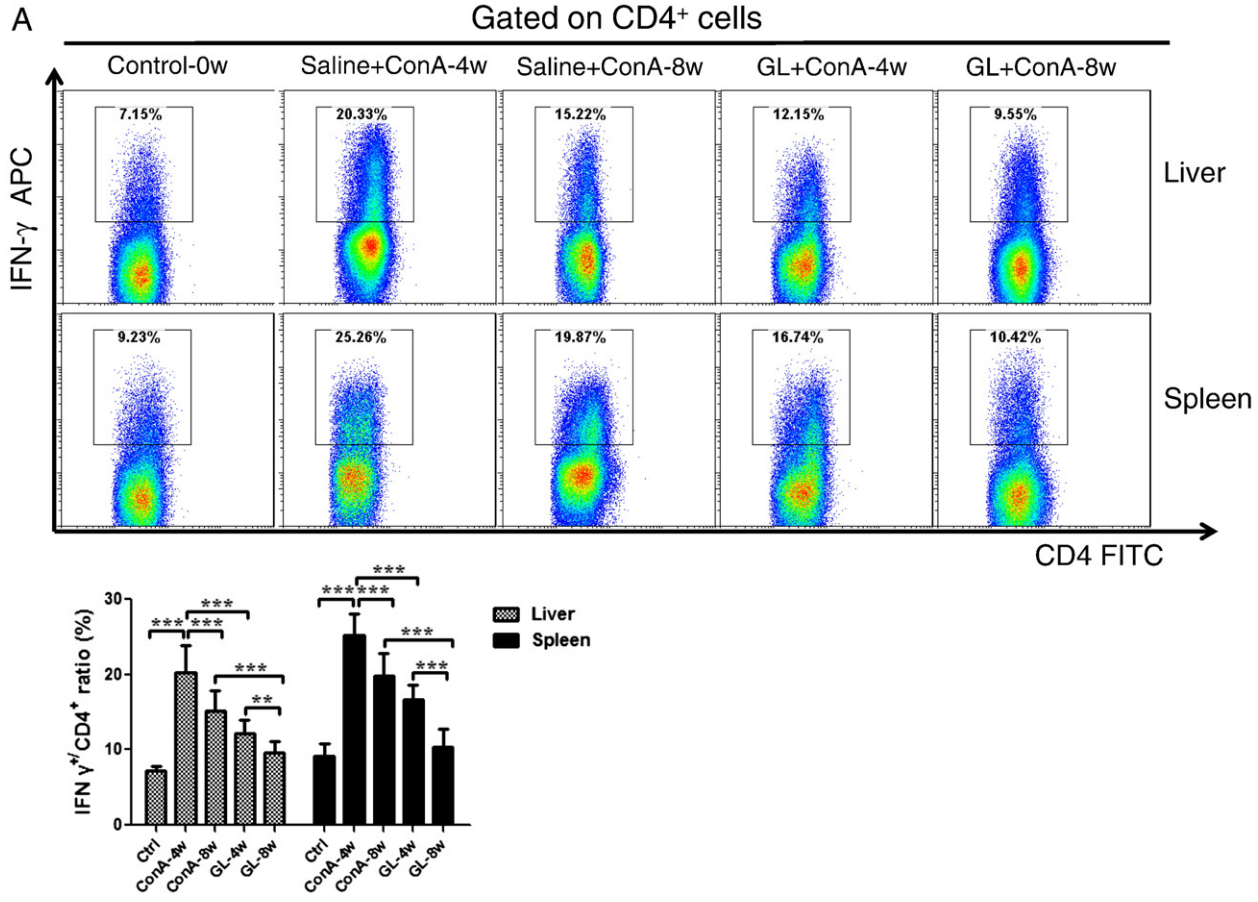

Fig. 2. Glycyrrhizin (GL) alters $CD4^+$T cell response in livers and spleens of ConA-induced mouse liver fibrosis models. Non-parenchymal cells in mouse livers and spleens were isolated to be analyzed by flow cytometry. (A–D) Representative infiltrations of $CD4^+$IFN-γ^+ cells (Th1), $CD4^+$IL-4^+ cells (Th2), $CD4^+$Foxp3^+ cells (Tregs) and $CD4^+$IL-17^+ cells (Th17) in mouse livers and spleens at week 4, 8 after ConA or ConA + 50 mg/kg GL treatments are presented on the left side with pooled data on the right side. ($^*p<0.05$, $^{**}p<0.01$, $^{***}p<0.001$. n = 10 per group).

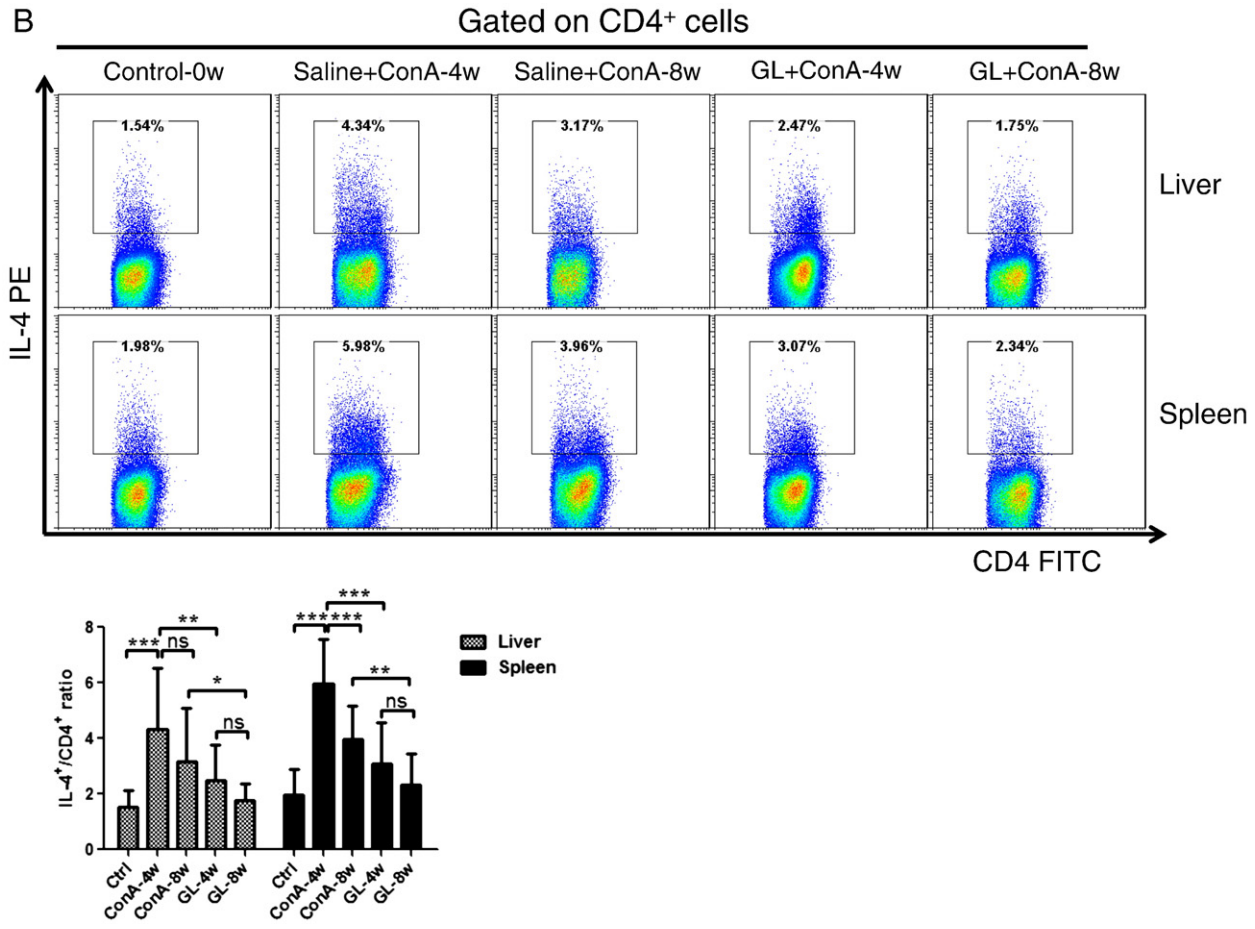

Fig. 2 (*continued*).

of counts per minute (cpm) for cells exposed to antigen divided by the mean number of cpm for cells not exposed to antigen.

2.8. Quantitative reverse transcriptase-PCR (qPCR)

Total RNA was extracted using TRIzol (Invitrogen). Following the manufacturer's instructions, reverse transcription was performed using a PrimeScript RT reagent kit with gDNA Eraser (Takara, Beijing, China) and quantitative real-time PCR conducted with a SYBR reverse transcription-polymerase chain reaction Kit (Takara) using the following conditions: 30 s at 95 °C, followed by a total of 40 two-temperature cycles (5 s at 95 °C and 30 s at 60 °C). Each assay was performed in triplicate. The primer sequences used were shown in Table 1. For analysis, the expression of target genes was normalized by the housekeeping gene GAPDH. Based on the ΔΔCt method, relative amounts of mRNA were expressed as $2^{-\Delta\Delta Ct}$.

2.9. Western blotting

Liver samples were homogenized and centrifuged at 10,000 *g* at 4 °C for 10 min. Cells were washed twice with ice-cold PBS and prepared with RIPA buffer (50 mM Tris–HCl, 150 mM NaCl, 1% Nonidet P-40, 0.5% deoxycholate and 0.1% SDS) containing protease inhibitor mixture (Roche). The samples were separated by SDS-PAGE and then transferred onto a polyvinylidenedifluoride membrane (Millipore, Billerica, MA, USA) using SemiDry Transfer Cell (Bio-Rad, Hercules, CA, USA). The polyvinylidenedifluoride membrane was blocked with 5% non-fat milk for 3 h followed by incubation with primary antibody in TBST (100 mM Tris–HCl, pH 7.5, 0.9% NaCl, 0.1% Tween 20) overnight at 4 °C with gentle shaking: the specific primary antibodies against α-SMA (1:1000, Sigma-Aldrich, St. Louis, MO, USA), against ERK (1:1000), against p-ERK (1:1000), against AKT (1:500), against p-AKT (1:500), against JNK (1:500), against p-JNK (1:1000), against p38 (1:200) and against p-p38 (1:1000). All the antibodies except α-SMA antibody were purchased from Abcam Inc., (Cambridge, MA). The blots were incubated with an HRP-conjugated anti-GAPDH antibody (1:10,000; KC5G5, CHN) for 1 h at room temperature. The ratio of each protein to GAPDH was calculated as the relative quantification.

2.10. Inhibition experiment

Splenic $CD4^+$T cells were incubated with LY294002 (PI3K/AKT inhibitor, 25 mM, Promega, Madison, WI, USA), U0126 (ERK inhibitor, 150 nM, Promega), SB203580 (p38 inhibitor, 1 mM, Promega) and SP600125 (JNK inhibitor, 100 nM, Sigma-Aldrich, St. Louis, MO, USA) for 1 h, and then ConA (10 μg/mL) was added to culture medium of each group. After 72 h of incubation, cell proliferation was measured by the thymidine method and cytokine secretion was measured by qPCR according to the above methods.

2.11. Statistical analysis

Results are presented as mean ± standard error of the mean (SEM) in triplicate. Statistical analyses were performed using the GraphPad Software Version 5.01 (CA, USA). Student's *t*-test and one-way ANOVA, χ^2 test and Pearson's rank correlation were performed as

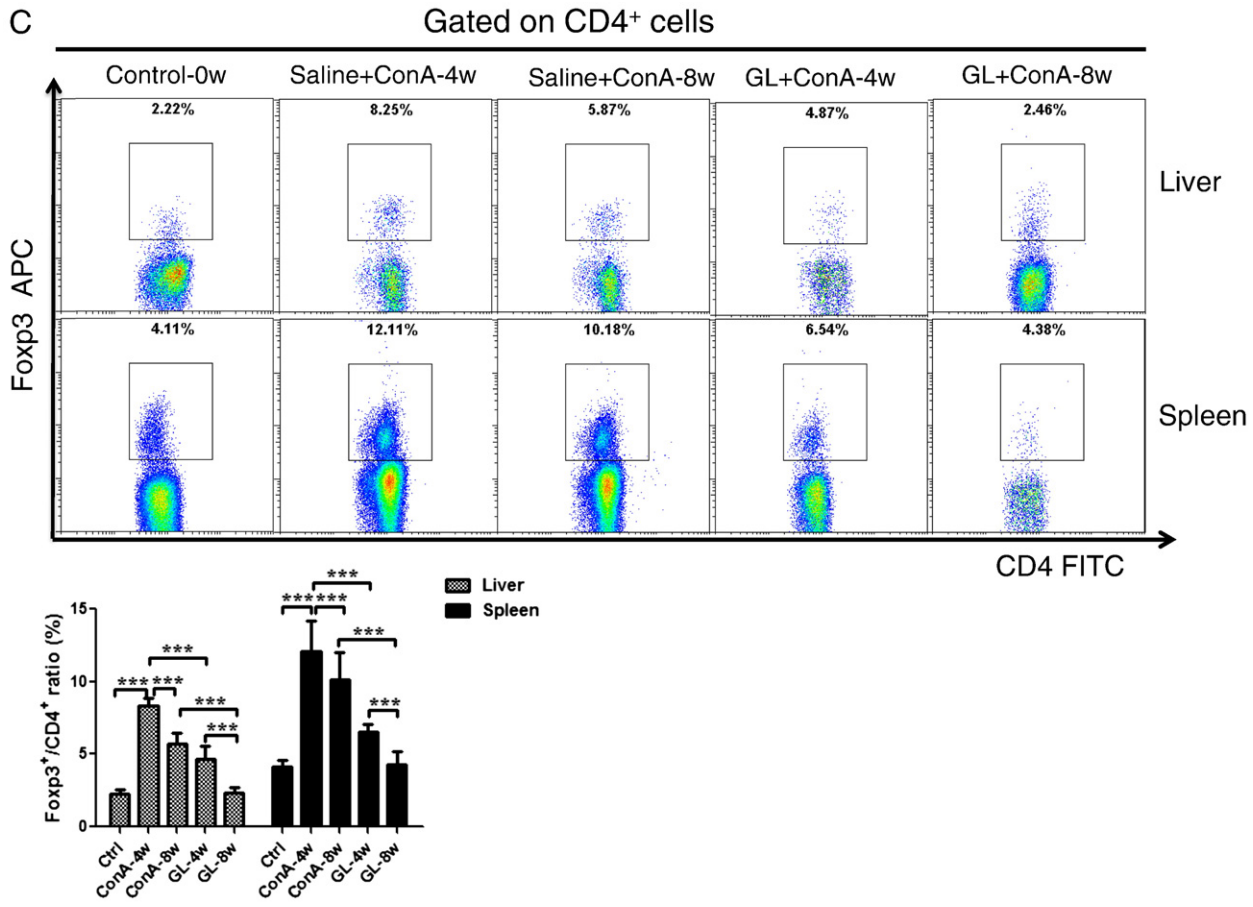

Fig. 2 (*continued*).

appropriate, and *p* values of less than 0.05 (two-tailed) were considered statistically significant.

3. Results

3.1. GL administration ameliorates ConA-induced hepatic injury, inflammation and fibrosis in mouse models

After ConA administration, mice developed significant hepatic inflammation, hepatocyte ballooning, necrosis, and distorted hepatic architectural formation as shown in H&E staining of liver tissue (Fig. 1A). At the end of 8 weeks after ConA administration, extension of fiber cable and formation of hepatic lobule were observed and very few areas of healthy hepatocytes and collagen deposition with septa bridging portal regions was detected (Fig. 1A). In line with these changes, serum ALT levels (as an indicator of hepatic inflammation) were much higher in ConA-induced fibrosis mice than PBS-treated mice at week 8 (Fig. 1B). However, administration of GL to ConA-treated mice significantly alleviated hepatic inflammation and necrosis, especially at high-dose (Fig. 1A and B).

Next, we investigated liver fibrosis degree of mice in differently-treated groups via Masson staining, a qualitative assessment of liver fibrosis. At week 8 after weekly ConA injections, the fibrosis scores of the three GL-treated groups were significantly lower than those of ConA-treated group (Fig. 1C). These results indicated that GL improved ConA-induced liver inflammation and fibrosis.

Because HSCs are the main collagen-producing cells in liver fibrosis, we analyzed activated HSCs via immunohistochemical staining for α-SMA expression. We observed α-SMA in all groups of animals, with the highest intensity in mice injected with ConA alone, with administration of GL significantly decreasing the levels of α-SMA expression (Fig. 1A). These findings were substantiated by real-time PCR and Western blot analyses which showed that both mRNA and protein levels of α-SMA were significantly reduced following GL treatment (Fig. 1D and E).

3.2. GL alters the proportion and balance of hepatic and splenic CD4$^+$T cells upon ConA induced liver fibrosis in mice

To assess the effects of GL on CD4$^+$T response during liver fibrosis, the proportion of infiltrating CD4$^+$IFN-γ$^+$ cells (Th1), CD4$^+$IL-4$^+$ cells (Th2), CD4$^+$Foxp3$^+$ cells (Tregs) and CD4$^+$IL-17$^+$ cells (Th17) cells were analyzed in livers and spleens of ConA-induced mouse liver fibrosis models with or without GL treatment. ConA induced a significant infiltration of Th1 cells in livers and spleens with progressed fibrosis degree in mouse models (Fig. 2A). ConA also induced dramatic increases of Th2, Tregs and Th17 in mouse livers and spleens (Fig. 2B–D). The peak infiltrating time point for Th1, Th2 and Tregs is week 4 after ConA administration, and then the proportions of the three subsets began to decrease, however, still with a higher level than untreated Balb/c mice (Fig. 2A–C). But the infiltration of Th17 peeked at week 8 (Fig. 2D). With administration of GL in ConA-induced mouse liver fibrosis models, the infiltration of Th1, Treg, Th17 and Th2 lineages were dramatically decreased compared to those treated with saline as a control, especially those treated with high dose of GL (Fig. 2).

Furthermore, GL dramatically increased the Th1/Th2 and Treg/Th17 ratios in livers and spleens in mouse models (Fig. 3).

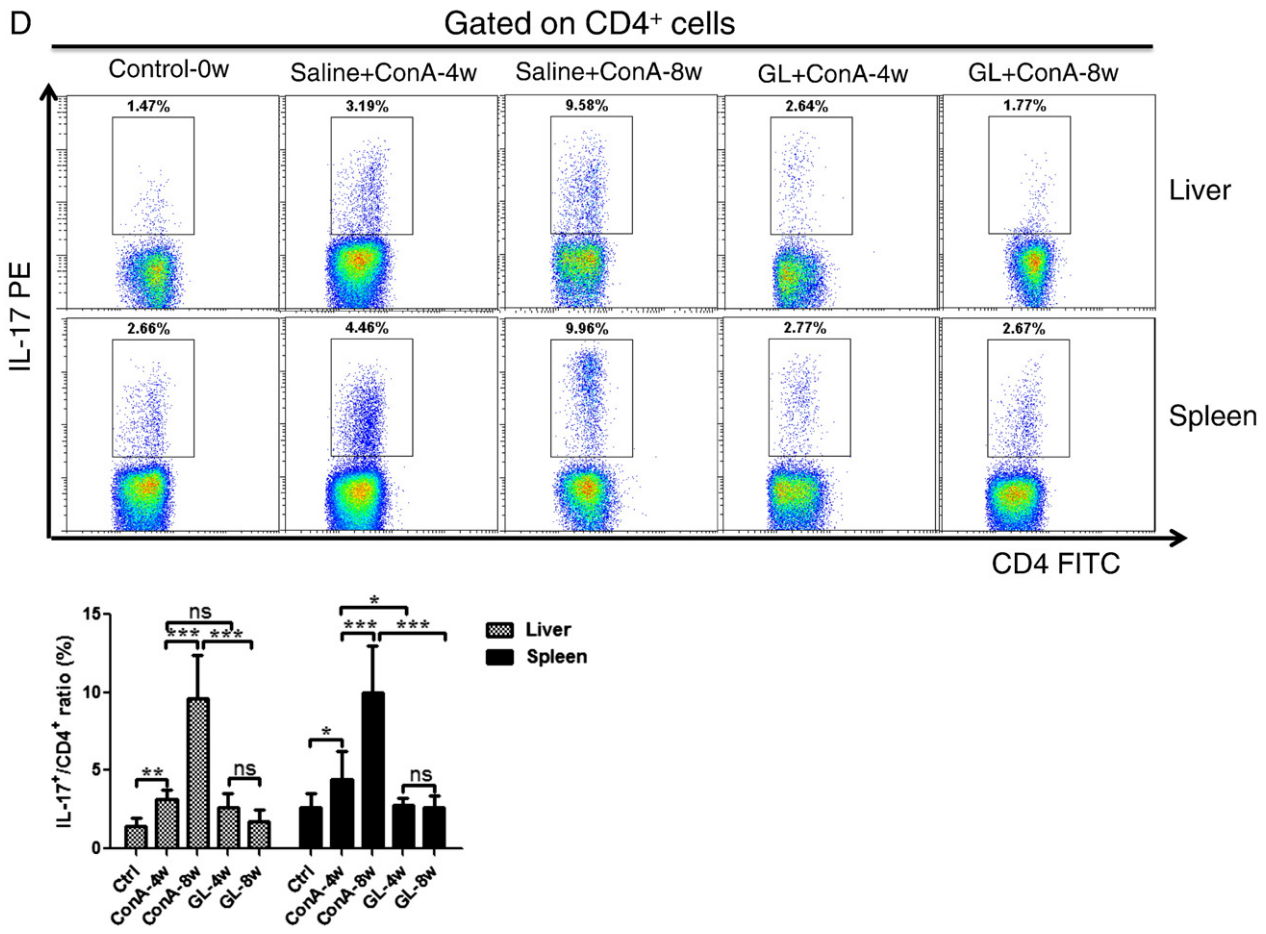

Fig. 2 (*continued*).

3.3. GL inhibits ConA-induced proliferation of splenic CD4$^+$T cells in vitro

Cell proliferation assay could be used to evaluate T-cell status, so we determined the effects of GL on splenic CD4$^+$T cell proliferation. Firstly, to assess the effects of ConA on CD4$^+$T cell proliferation, we co-cultured 10 μg/mL ConA with splenic CD4$^+$T cells isolated from Balb/c mice for 0, 12, 24, 48, and 72 h. The proliferation of splenic CD4$^+$T cells was measured by the thymidine method. As shown in Fig. 4A, ConA promoted the proliferation of splenic CD4$^+$T cells with the prolonged time and peaked at 48–72 h. Secondly, to assess the effects of treatment with GL on the immune response in the ConA stimulated splenic CD4$^+$T cell proliferation, different concentrations (0, 5, 10, 100 μg/mL) of GL were added into the culture medium for 72 h. As shown in Fig. 4B, GL significantly inhibited ConA-induced T cell proliferation in a dose-dependent manner.

3.4. JNK, ERK and PI3K/AKT signaling molecules were involved in proliferation of ConA-stimulated CD4$^+$T cells

To identify the signaling pathways involved in ConA-stimulated CD4$^+$T proliferation, the pharmacological inhibitors of MAPK and PI3K/AKT were used in this part of study. CD4$^+$T cells pretreated with LY294002 (PI3K/AKT inhibitor), U0126 (ERK inhibitor), SB203580 (p38 inhibitor) and SP600125 (JNK inhibitor) for 1 h were incubated with ConA for 72 h. As shown in Fig. 4C, the proliferation of CD4$^+$T cells induced by ConA can be significantly inhibited by LY294002, U0126 and SP600125, but not the p38 inhibitor SB203580 (Fig. 4C).

3.5. GL influenced the expression of JNK, ERK and PI3K/AKT signaling molecules on ConA stimulated CD4$^+$T cells

To investigate the potential mechanisms for GL to regulate ConA-induced CD4$^+$T cell proliferation, we assessed the protein levels of JNK, ERK and PI3K/AKT in CD4$^+$T cells after the co-treatment of ConA and GL. First, we incubated freshly isolated splenic CD4$^+$T cells from normal Balb/c mice with 10 μg/mL ConA for 0, 12, 24, 48 and 72 h; and detected the protein levels of AKT, ERK, JNK, P38 and their respective active forms (p-AKT, p-ERK, p-JNK and p-P38) in these cells by western blot. We found the proteins of p-JNK, p-ERK and p-AKT on T cells significantly increased in response to ConA incubation; however no change of p-P38 was detected (Fig. 5A and B). Second, we added GL at diverse concentrations (0, 10, 100 μg/mL) into the culture medium and incubated ConA-stimulated CD4$^+$T cells with GL for 72 h. As shown in Fig. 5C and D, GL treatment significantly decreased the enhancement of p-JNK, p-ERK and p-AKT in response to ConA in CD4$^+$T cells.

3.6. GL increases the expression of anti-fibrotic cytokines in livers of ConA-induced fibrosis models

We also investigated the effects of GL on anti-fibrotic cytokines in livers of ConA-induced mouse models. Since CD4$^+$T cells usually produce abundant cytokines to regulate fibrosis progression, we analyzed the mRNA expression of cytokines IL-10, IFN-γ, IL-13 and TGF-β1, which are mainly produced by CD4$^+$T cells and with a close

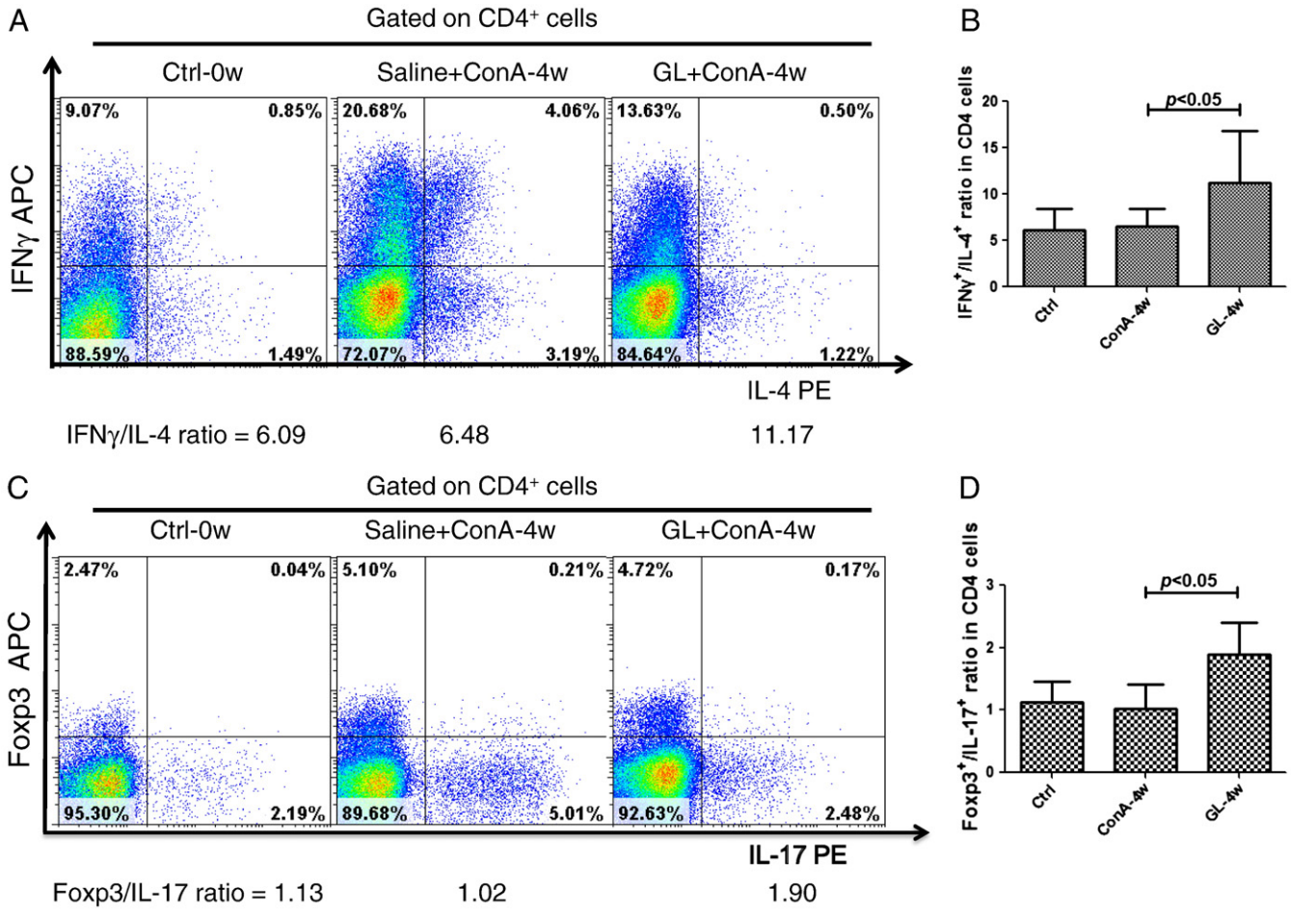

Fig. 3. Glycyrrhizin (GL) administration regulates intrahepatic Th1/Th2 and Treg/Th17 balance in ConA-induced mouse liver fibrosis models. (A, B) GL treatment could significantly increase the Th1/Th2 ratio in liver tissues at week 4 with pooled data as mean ± SEM (n = 10 per group) are on the right side.(C, D) GL treatment could also dramatically increase the hepatic Treg/Th17 ratio and pooled data as mean ± SEM (n = 10 per group) are on the right side.

link with the fibrogenesis after GL treatment. We found that GL administration significantly enhanced the mRNAs of anti-fibrotic IL-10 and IFN-γ (Fig. 6A), however not the pro-fibrotic IL-13 and TGF-β1 (Fig. 6B).

3.7. GL alters IFN-γ and IL-10 mRNAs of splenic CD4$^+$T cells in vitro not via JNK, ERK and PI3K/AKT signaling pathways

We also confirmed in vitro that GL could significantly enhance the IFN-γ and IL-10 mRNAs in splenic CD4$^+$T cells and found that the enhancement of IFN-γ and IL-10 by GL treatment was not via JNK, ERK and PI3K/AKT signaling pathways with the co-incubation of pharmacological inhibitors of MAPK and PI3K/AKT(Fig. 6C).

4. Discussion

Liver cirrhosis, the common clinical endpoint of chronic liver diseases, is characterized by tissue fibrosis, replacement of normal liver architecture by structurally abnormal nodules and the development of portal hypertension and other life-threatening complications [1–3]. Inhibition of fibrogenesis at an early stage is nowadays considered as a feasible strategy to treat liver cirrhosis [2,4].

In this study, using ConA-induced mouse liver fibrosis models, we found that glycyrrhizin (GL) significantly attenuated fibrosis progression. GL not only reduced liver inflammation, but significantly suppressed the activation of HSCs and reduced collagen accumulation in mice (Fig. 1). These changes were accompanied by the down-regulation of CD4$^+$T cells infiltration in the livers and spleens of mice with hepatic fibrosis (Figs. 2 and 3).

GL is a natural anti-inflammatory and antiviral triterpene to treat patients with viral hepatitis (hepatitis B and hepatitis C) and to reduce the risk of hepatocellular carcinoma after hepatitis-C virus (HCV) infection in China and Japan [22–27,32]. GL could also inhibit the cytotoxicity mediated by CD4$^+$T cells and TNF [33]. GL has a membrane stabilizing effect [34] and also stimulates endogenous production of interferon [21,25,26]. 18-β GL shows an antiviral activity against a great deal of DNA and RNA viruses due to potential activation of NF-κB and induction of IL-8 secretion [35]. 18-α GL is also reported to suppress the activation of HSCs and induce the apoptosis of HSCs by blocking the translocation of NF-κB to the nucleus [36]. However, abundant basic and clinical studies are still needed to further clarify pharmacological effects of GL, before it's included in the treatment of liver fibrosis.

Here, our study provides new insights of the anti-inflammatory and anti-fibrotic effects of GL in ConA-induced mouse models. Our data have indicated that GL exert its therapeutic effects partly by regulating the infiltration of CD4$^+$T cells in livers (Figs. 2 and 3). GL treatment not only decreased the proportions of all the four major CD4$^+$T cell lineages including Treg, Th17 and Th2 and Th1 but also increased the ratios of Th1/Th2 and Treg/Th17, indicating a dominance of Th1 and Treg among infiltrating CD4$^+$T cells (Figs. 2 and 3). The outcome of immune reaction is determined by the balance between

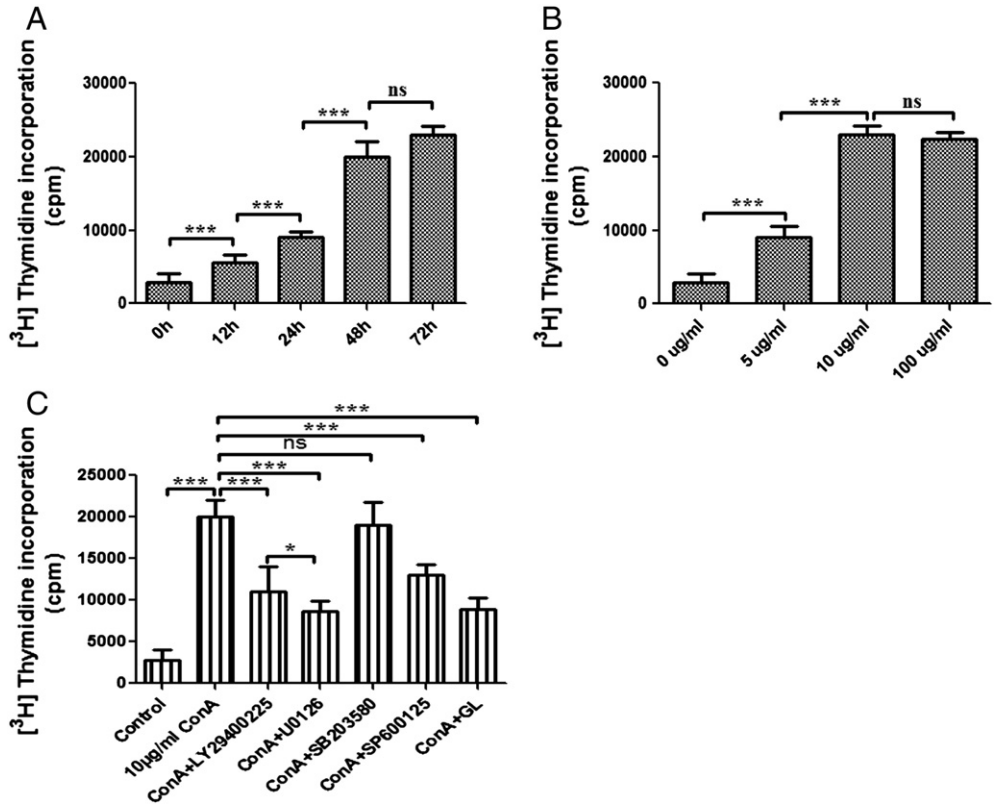

Fig. 4. Glycyrrhizin (GL) inhibits ConA-induced proliferation of splenic CD4$^+$T cells. The proliferations of splenic CD4$^+$T cells were assessed by ^{3}H-thymidine method. (A) The proliferation of splenic CD4$^+$T cells isolated from Balb/c mice was detected after the incubation with ConA (10 μg/mL) for 0, 12, 24, 48 and 72 h. (B) Effects of GL treatment on ConA-stimulated proliferation of splenic CD4$^+$T cells at different concentrations (0, 10, 100 μg/mL) for 72 h are shown. (C) The proliferation of CD4$^+$ cells pretreated with GL (10 μg/mL), LY294002 (PI3K/AKT inhibitor), U0126 (ERK inhibitor), SB203580 (p38 inhibitor) or SP600125 (JNK inhibitor) for 1 h was analyzed after their incubations with ConA for 72 h.

pro-inflammation and anti-inflammation. The discovery of functional CD4$^+$T cell lineages calls for the concept of CD4$^+$T cell balance (the balance between different functional lineages). In our study, ConA induced a significantly increased infiltrating Th1, Th2, Tregs and Th17 lineages in livers and spleens of mouse models (Fig. 2). The cytokines mainly produced by CD4$^+$T cells were also shaped by ConA administration (Fig. 6). These findings indicated that CD4$^+$T cell responses are involved in ConA-induced liver fibrosis. Using the above mouse models, we also demonstrated that GL could significantly inhibit ConA-induced CD4$^+$T cell infiltration and alter the mode of cytokine production, thus proving the immunoregulatory effects of GL on liver fibrosis progression. The role of CD4$^+$Th2 cells and STAT6-mediated signaling pathway in the development of fibrosis has been well documented in several studies performed in animal models, such as the tight skin (TSK) mouse. Th2-dominated responses play a crucial role in the pathogenesis of a variety of fibrotic diseases [37]. Previous studies also showed that perturbations in the Th1/Th2 cytokine balance can significantly affect the extent of tissue fibrosis in *S. mansoni*-infected mice [38]. Besides, intrahepatic Treg plays a dual role in obstructive jaundice for suppressing T cell function while limiting cholestasis and hepatic fibrosis [39].

Hepatic fibrosis secondary to most chronic liver diseases is always driven by the repair responses to injured tissues. During chronic hepatic inflammation, CD4$^+$T cells as well as other immune cells produce abundant cytokines to indirectly modulate the behavior of quiescent HSCs [38–40]. ConA, a legume lectin, is a mitogen for monocytes, T-cells, splenocytes, and other cells. The administration of ConA to mice triggers T-cell activation, and the following release of pro-inflammatory cytokines such as IFN-γ and TNF-α, which contribute to chronic inflammation and following fibrogenesis [37,41]. GL has been reported to prevent ConA induced mouse liver injury without affecting the production of cytokines such as IFN-γ and TNF-α [42]. However, there is also evidence that the production of IL-6 and IL-10 in the livers of ConA-treated mice is suppressed by GL treatment [32]. Another report has shown that GL inhibits increased IL-18 and matrix metalloproteinase-9 production in mice treated with LPS/GalN [40,41]. GL also enhances IL-10 production by hepatic dendritic cells in mice with hepatitis [43]. Here, we detected mRNAs of several fibrosis-related cytokines mainly produced by CD4$^+$T cells in ConA-induced fibrosis mice with or without GL treatment, and found that GL dramatically increased the mRNAs of IL-10 and IFN-γ, however, not the mRNAs of IL-13 and TGF-β1. To coincide with our data, other researchers found that disease progression in CCl4-induced mouse liver fibrosis models is associated with increased IL-4 and decreased IFN-γ, respectively produced by CD4$^+$Th2 and CD4$^+$Th1 cells [12]. Thus, intrahepatic CD4$^+$T cells produce high levels of immunomodulatory cytokines and are involved in liver inflammation and fibrosis by regulating HSC activation.

To investigate further the molecular mechanism underlying the ability of GL to suppress the proliferation of CD4$^+$T cells induced by ConA, we co-cultured GL with ConA-stimulated splenic CD4$^+$T cells for further research. We found that GL, especially high dose, inhibited the increased proliferation and modulated the inflammatory cytokines of splenic CD4$^+$T cells stimulated with ConA significantly (Figs. 4 and 6).

Numerous reports have demonstrated that MAPK member which includes p42/44, p38, and JNK, and PI3K-dependent pathway are involved in cell growth, differentiation as well as apoptosis [19,20]. MAPK and PI3K pathways also play an important regulator in the proliferation and migration of T cells [19,20]. In this study, we aimed to

investigate whether JNK, ERK and PI3K/AKT were involved in the process for GL to inhibit ConA-induced CD4$^+$T cell proliferation, and found that phosphorylation of JNK, ERK and AKT not p38 in CD4$^+$T cells significantly increased after ConA treatment which could be inhibited by the co-incubation of GL in vitro in a dose- and time-dependent manner (Fig. 5). The results demonstrated that treatment with GL inhibited ERK, JNK, PI3K and Akt phosphorylation significantly, indicating GL's ability to regulate CD4$^+$T cells via JNK, ERK and PI3K/AKT signaling pathways. The results also indicated that ERK, JNK and PI3K/Akt pathways may be the potential targets for inhibiting liver fibrosis progression. Similarly, phosphorylation of JNK, ERK and AKT was induced by ConA, and inhibitors of JNK, ERK and PI3K/AKT significantly decreased the HBcAg-induced PD-1 upregulation on CD4$^+$T cells [44].

In conclusion, GL alleviated ConA-induced inflammation and fibrosis progression in livers of mouse models via the inhibition of CD4$^+$T cell proliferation in response to ConA via JNK, ERK and PI3K/AKT pathway.

Competing interests

The authors declare that they have no competing interests.

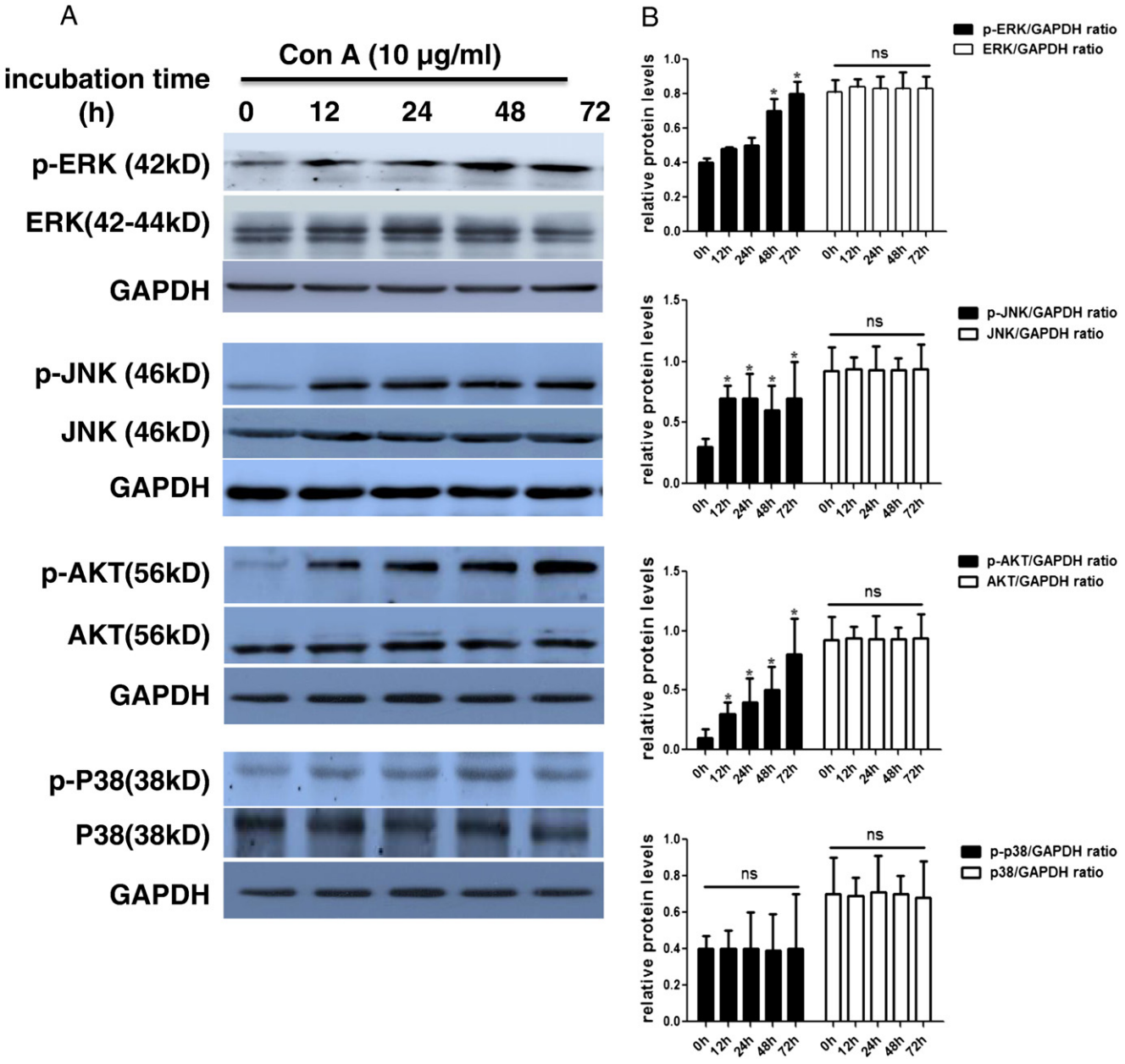

Fig. 5. Glycyrrhizin (GL) treatment in vitro down-regulates ConA-enhanced expression of p-JNK, p-ERK and p-AKT in CD4$^+$ cells. (A) Splenic CD4$^+$T cells were stimulated with ConA (10 μg/mL) for 12, 24, 48 and 72 h to be analyzed the protein levels of ERK/phosphorylation (p)-ERK, JNK/p-JNK, AKT/p-AKT and P38/p-P38 by western blot. (B) Relative quantification of the total and active forms of JNK, ERK, PI3K/AKT and p38 proteins are presented. *$p<0.05$ vs 0 h. (C) Splenic CD4$^+$T cells were stimulated with ConA (10 μg/mL) for 72 h and then with different concentrations of GL for 72 h to be analyzed the proteins of p-ERK, p-JNK and p-AKT by western blot. Results are representative of three independent experiments. (D) Relative quantification of the total and active forms of JNK, ERK and PI3K/AKT proteins are presented. *$p<0.05$ vs 0 μg/mL GL group.

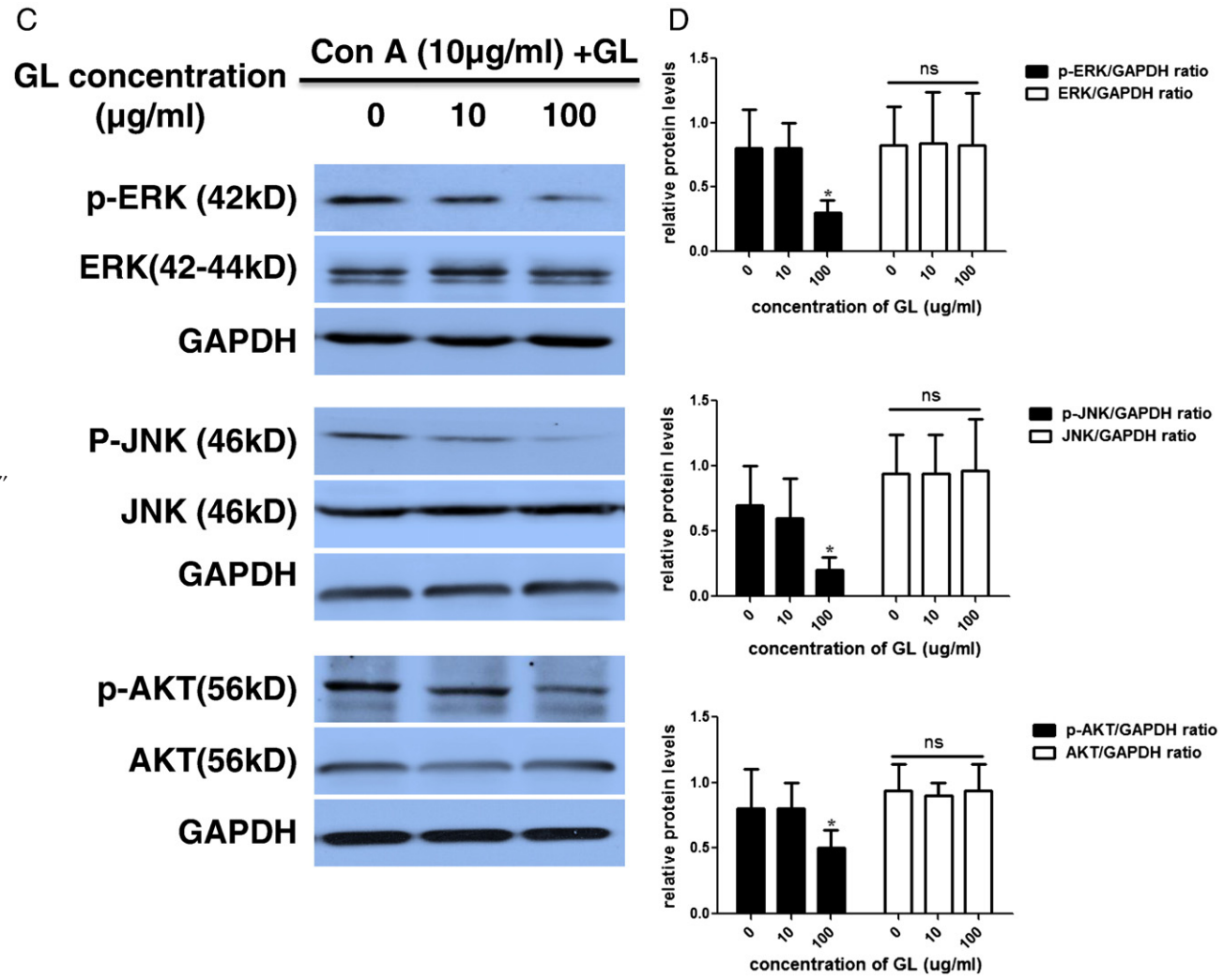

Fig. 5 (*continued*).

References

[1] Iredale JP. Models of liver fibrosis: exploring the dynamic nature of inflammation and repair in a solid organ. J Clin Invest 2007;117:8–539.
[2] Friedman SL. Mechanisms of hepatic fibrogenesis. Gastroenterology 2008;134: 1655-69.
[3] Leask A, Abraham DJ. TGF-beta signaling and the fibrotic response. FASEB J 2004;18:816-27.
[4] Lee UE, Friedman SL. Mechanisms of hepatic fibrogenesis. Best Pract Res Clin Gastroenterol 2011;25:195-206.
[5] Hashimoto N, Shimoda S, Kawanaka H, Tsuneyama K, Uehara H, Akahoshi T, et al. Modulation of CD4 T cell responses following splenectomy in hepatitis C virus-related liver cirrhosis. Clin Exp Immunol 2011;165:243-50.
[6] Heymann F, Hammerich L, Storch D, Bartneck M, Huss S, Rüsseler V, et al. Hepatic macrophage migration and differentiation critical for liver fibrosis is mediated by the chemokine receptor C-C motif chemokine receptor 8 in mice. Hepatology 2012;55:898-909.
[7] Karlmark KR, Wasmuth HE, Trautwein C, Tacke F. Chemokine-directed immune cell infiltration in acute and chronic liver disease. Expert Rev Gastroenterol Hepatol 2008;2:233-42.
[8] Littman DR, Rudensky AY. Th17 and regulatory T cells in mediating and restraining inflammation. Cell 2010;140:845-58.
[9] Miossec P, Korn T, Kuchroo VK. Interleukin-17 and type 17 helper T cells. N Engl J Med 2009;361:888-98.
[10] Winau F, Quack C, Darmoise A, Kaufmann SH. Starring stellate cells in liver immunology. Curr Opin Immunol 2008;20:68-74.
[11] Vinas O, Bataller R, Sancho-Bru P, Gines P, Berenguer C, Enrich C, et al. Human hepatic stellate cells show features of antigen-presenting cells and stimulate lymphocyte proliferation. Hepatology 2003;38:919-29.
[12] Bot A. Immunoglobulin deficient mice generated by gene targeting as models for studying the immune response. Int Rev Immunol 1996;13:327-40.
[13] Marra F, Aleffi S, Galastri S, Provenzano A. Mononuclear cells in liver fibrosis. Semin Immunopathol 2009;31:345-58.
[14] Peng G, Li S, Wu W, Sun Z, Chen Y, Chen Z. Circulating $CD4^{+}CD25^{+}$ regulatory T cells correlate with chronic hepatitis B infection. Immunology 2008;123:57-65.
[15] Zhang JY, Zhang Z, Lin F, Zou ZS, Xu RN, Jin L, et al. Interleukin-17-producing CD4 (+) T cells increase with severity of liver damage in patients with chronic hepatitis B. Hepatology 2010;51:81-91.
[16] Weaver CT, Hatton RD. Interplay between the TH17 and TReg cell lineages: a (co-) evolutionary perspective. Nat Rev Immunol 2009;9:883-9.
[17] Zhang JY, Song CH, Shi F, Zhang Z, Fu JL, Wang FS. Decreased ratio of Treg cells to Th17 correlates with HBV DNA suppression in chronic hepatitis B patients undergoing entecavir treatment. PLoS One 2010;5:e13869.
[18] Niu YH, Liu HL, Yin DL, Yi RT, Chen TY, Xue H, et al. The balance between intrahepatic IL-17^{+} T cells and $Foxp3^{+}$ regulatory T cells plays an important role in HBV-related end-stage liver disease. BMC Immunol 2011;12:47-55.
[19] Plotnikov A, Zehorai E, Procaccia S, Seger R. The MAPK cascades: signaling components, nuclear roles and mechanisms of nuclear translocation. Biochim Biophys Acta 2011;1813:1619-33.
[20] Wang X, Hao J, Metzger DL, Ao Z, Chen L, Ou D, et al. B7-H4 treatment of T cells inhibits ERK, JNK, p38, and AKT activation. PLoS One 2012;7:e28232.
[21] Yamamura Y, Kotaki H, Tanaka N, Aikawa T, Sawada Y, Iga T. The pharmacokinetics of glycyrrhizin and its restorative effect on hepatic function in patients with chronic hepatitis and in chronically carbon-tetrachloride-intoxicated rats. Biopharm Drug Dispos 1997;18:717-25.
[22] Arase Y, Ikeda K, Murashima N, Chayama K, Tsubota A, Koida I, et al. The long term efficacy of glycyrrhizin in chronic hepatitis C patients. Cancer 1997;79: 1494-500.
[23] Sato H, Goto W, Yamamura J, Kurokawa M, Kageyama S, Takahara T, et al. Therapeutic basis of glycyrrhizin on chronic hepatitis B. Antiviral Res 1996;30:171-7.
[24] Fiore C, Eisenhut M, Krausse R, Ragazzi E, Pellati D, Armanini D, et al. Antiviral effects of Glycyrrhiza species. Phytother Res 2008;22:141-8.
[25] Stickel F, Schuppan D. Herbal medicine in the treatment of liver diseases. Dig Liver Dis 2007;39:293-304.
[26] Seeff LB, Lindsay KL, Bacon BR, Kresina TF, Hoofnagle JH. Complementary and alternative medicine in chronic liver disease. Hepatology 2001;34:595-603.

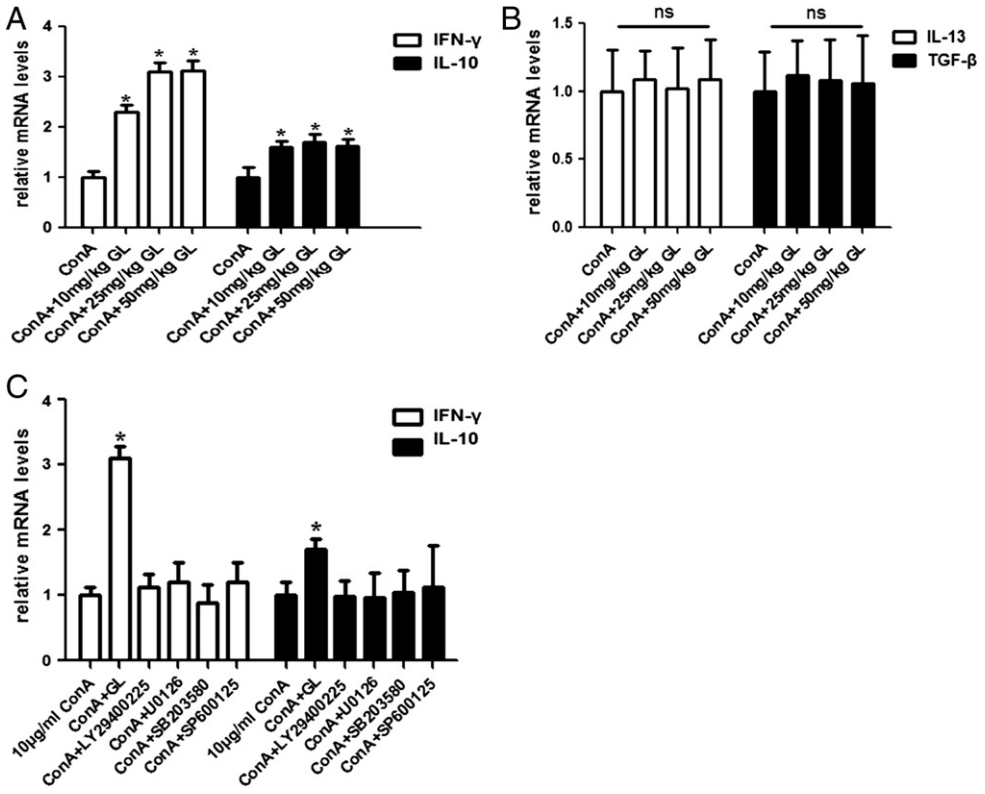

Fig. 6. Glycyrrhizin (GL) administration enhances mRNAs of intrahepatic IFN-gamma and IL-10 in ConA-induced mouse fibrosis models, however not via JNK, ERK and PI3K/AKT pathways. (A) GL administration significantly induced the expression of anti-fibrotic cytokines IL-10 and IFN-γ mRNAs in ConA-induced fibrosis models. (B) GL administration did not influence the mRNAs of IL-13 and TGF-β1. (C) Freshly-isolated splenic $CD4^+$T cells from normal Balb/c mice were cultured in medium alone or with ConA, GL, LY29400225 (PI3K/AKT inhibitor), U0126 (ERK inhibitor), SB203580 (p38 inhibitor) and SP600125 (JNK inhibitor) to be analyzed cytokines IL-10 and IFN-r mRNA by real-time PCR. Data are shown as the ratio of stimulated splenic $CD4^+$T cells to control cells in triplicate (n = 6).*$p<0.05$ vs ConA group.

[27] Ikeda M, Fujiyama S, Tanaka M, Sata M, Ide T, Yatsuhashi H, et al. Clinical features of hepatocellular carcinoma that occur after sustained virological response to interferon for chronic hepatitis C. J Gastroenterol Hepatol 2006;21:122-8.
[28] Wang JY, Guo JS, Li H, Liu SL, Zern MA. Inhibitory effect of glycyrrhizin on NF-kappaB binding activity in CCl4- plus ethanol-induced liver cirrhosis in rats. Liver 1998;18:180-5.
[29] Zhang Y, Li P, Li G, Huang X, Meng Q, Lau WY. The mechanism of how anti-IL-18 prevents concanavalin-A-induced hepatic fibrosis on a mouse model. J Surg Res 2007;142:175-83.
[30] Jonsson JR, Clouston AD, Ando Y, Kelemen LI, Horn MJ, Adamson MD, et al. Angiotensin-converting enzyme inhibition attenuates the progression of rat hepatic fibrosis. Gastroenterology 2001;121:148-55.
[31] Fan Y, Weifeng W, Yuluan Y, Qing K, Yu P, Yanlan H. Treatment with a neutralizing anti-murine interleukin-17 antibody after the onset of coxsackievirus b3-induced viral myocarditis reduces myocardium inflammation. Virol J 2011;14:8–17.
[32] Feng C, Wang H, Yao C, Zhang J, Tian Z. Diammoniumgly-cyrrhizinate, a component of traditional Chinese medicine Gan-Cao, prevents murine T-cell-mediated fulminant hepatitis in IL- 10- and IL-6-dependent manners. Int Immunopharmacol 2007;7:1292-8.
[33] Yoshikawa M, Matsui Y, Kawamoto H, Umemoto N, Oku K, Koizumi M, et al. Effects of glycyrrhizin on immune-mediated cytotoxicity. J Gastroenterol Hepatol 1997;12:243-8.
[34] Shiki Y, Shirai K, Saito Y, Yoshida S, Mori Y, Wakashin M. Effect of glycyrrhizin on lysis of hepatocyte membranes induced by anti-liver cell membrane antibody. J Gastroenterol Hepatol 1992;7:12-6.
[35] Shaneyfelt ME, Burke AD, Graff JW, Jutila MA, Hardy ME. Natural products that reduce rotavirus infectivity identified by a cell-based moderate-throughput screening assay. Virol J 2006;3:68.
[36] Qu Y, Chen WH, Zong L, Xu MY, Lu LG. 18α-glycyrrhizin induces apoptosis and suppresses activation of rat hepatic stellate cells. Med Sci Monit 2012;18: BR24-32.
[37] Siracusa LD, McGrath R, Ma Q, Moskow JJ, Manne J, Christner PJ, et al. A tandem duplication within the fibrillin 1 gene is associated with the mouse tight skin mutation. Genome Res 1996;6:300-13.
[38] Wynn TA, Cheever AW, Jankovic D, Poindexter RW, Caspar P, Lewis FA, et al. An IL-12-based vaccination method for preventing fibrosis induced by schistosome infection. Nature 1995;376:594-6.
[39] Katz SC, Ryan K, Ahmed N, Plitas G, Chaudhry UI, Kingham TP, et al. Obstructive jaundice expands intrahepatic regulatory T cells, which impair liver T lymphocyte function but modulate liver cholestasis and fibrosis. J Immunol 2011;187:1150-6.
[40] Heinrichs D, Knauel M, Offermanns C, Berres ML, Nellen A, Leng L, et al. Macrophage migration inhibitory factor (MIF) exerts antifibrotic effects in experimental liver fibrosis via CD74. Proc Natl Acad Sci USA 2011;108:17444-9.
[41] Fujikura S, Mizuhara H, Miyazawa Y, Fujiwara H, Kaneda K. Kinetics and localization of lymphoblasts that proliferate in the murine liver after Concanavalin A administration. Biomed Res 1996;17:129-39.
[42] Okamoto T, Kanda T. Glycyrrhizin protects mice from concanavalin A-induced hepatitis without affecting cytokine expression. Int J Mol Med 1999;4:149-52.
[43] Abe M, Akbar F, Hasebe A, Horiike N, Onji M. Glycyrrhizin enhances interleukin-10 production by liver dendritic cells in mice with hepatitis. J Gastroenterol 2003;38:962-7.
[44] Li M, Sun XH, Zhu XJ, Jin SG, Zeng ZJ, Zhou ZH, et al. HBcAg induces PD-1 upregulation on $CD4^+$T cells through activation of JNK, ERK and PI3K/AKT pathways in chronic hepatitis-B-infected patients. Lab Invest 2012;92:295-304.